Excitation functions of inelastic and transfer channels in $^{12}C+^{12}C$ around $E_{c.m.}=32.5$ MeV

S. Szilner and Z. Basrak
Centre de Recherche Nucléaires and Université Louis Pasteur, F-67037 Strasbourg Cedex 2, France
and Ruđer Bošković Institute, HR-10001 Zagreb, Croatia

R. M. Freeman, F. Haas, A. Morsad,* and C. Beck
Centre de Recherche Nucléaires and Université Louis Pasteur, F-67037 Strasbourg Cedex 2, France
(Received 16 October 1996)

A prominent and wide resonance centered at $E_{c.m.}=32.5$ MeV has recently been found in the $(0_2^+,0_2^+)$ inelastic channel of the $^{12}C+^{12}C$ reaction. It has been suggested that it corresponds to a 6α-particle-chain state in ^{24}Mg. In the present work we study $^{12}C+^{12}C$ excitation functions between center-of-mass energies of 30 and 35 MeV in steps of 250 keV for weakly populated outgoing channels. We present the inelastic channels to the states above the α-particle decay threshold, $(0_1^+,0_2^+)$, $(0_1^+,3_1^-)$, and $(0_1^+,4_1^+)$, and the one- and two-nucleon transfer channels. In the inelastic and the transfer channels we observe correlated intermediate-width structures at $E_{c.m.}=31$, 32.5, and 33.5 MeV, whose widths are appreciably smaller than the width measured in the $(0_2^+,0_2^+)$ channel. Our $E_{c.m.}=32.5$ MeV angular distribution of the $(0_1^+,0_2^+)$ channel exhibits oscillatory behavior and, unlike that of the $(0_2^+,0_2^+)$ channel, does not display enhancement around $\theta_{c.m.}=90°$. Data were collected via the kinematic coincidence technique. For data reduction we use a novel approach allowing for the extraction of results on nonbinary channels. [S0556-2813(97)01603-8]

PACS number(s): 25.70.Ef, 25.70.Hi, 27.30.+t

I. INTRODUCTION

The collision of carbon nuclei leading to the ^{24}Mg composite nucleus is by far the most studied light-heavy-ion reaction. This system shows an overwhelming amount of resonant structures ranging from deeply below the Coulomb barrier up to projectile energies that are a few times the barrier value [1–3]. The $^{12}C+^{12}C$ system continuously delivers surprises to the physics community. The recent discovery of the Argonne group reported evidence for a 6α-chain state at $E_{c.m.}=32.5$ MeV, i.e., at an excitation energy of 46.4 MeV in ^{24}Mg [4]. A claim for the existence of a stretched configuration of six aligned α particles is based on the observation of a strong structure of a textbook example for an isolated Breit-Wigner resonance in the angle-integrated cross section of the mutually inelastic scattering to 0_2^+ states in ^{12}C nuclei [4]. The 0_2^+ state at an excitation of 7.65 MeV in ^{12}C is well known as a state slightly above the 3α-particle decay threshold having a rather large deformation [5] to the point of predicting it as a 3α particle linear or bent, but close to the linear configuration [6–13]. The 6α-chain state would preferentially decay by fissioning into (two) 3α chains. The extreme deformation of ^{24}Mg was foreseen by the Nilsson-Strutinsky α-cluster model [14], by the rotational-vibrational model calculations using an anharmonic nucleus-nucleus potential [15], and by the cranked α-cluster model [16].

In addition to the great excitement aroused by the possible evidence of the extreme deformation of the ^{24}Mg nucleus, these data show a number of peculiarities. A few comments should be made on the $^{12}C[0_2^+]+^{12}C[0_2^+]$ inelastic data around 32.5 MeV [4] at their face value:

(i) A regular background-free Breit-Wigner shape for a resonance amplitude is an exception among heavy-ion resonances (see, e.g., Refs. [17,18]).

(ii) Such behavior suggests that this reaction populates a strong *isolated* resonance in ^{24}Mg.

(iii) A resonance width of 4.7 MeV is exceptionally large: it is by a factor of at least three larger than any isolated light-heavy-ion resonance reported so far.

(iv) The position of maxima and minima in the limited angular range covered by the setup is oscillatory and consistent with the squared Legendre polynomial of degree $l=14(16)$.

(v) In spite of the preceding feature, the on-resonance angular distributions show a very strong enhancement about 90°. The 90° maximum exceeds the neighboring maxima by a factor of 2 to 4.

(vi) The angular distributions were measured and integrated effectively only over 20°. (The measurement covered the angular range $70°\leqslant\theta_{c.m.}\leqslant105°$. Note the forward-backward symmetry required by the indistinguishability of identical bosons in the reaction entrance channel.)

(vii) Despite the strongly mismatched angular momenta of the entrance and the exit channels of 6 $\hbar$ units (spherical nuclei assumed), the reaction cross section is surprisingly large. The angle-averaged on-resonance cross section σ_{av} is 15 μb for $(0_2^+,0_2^+)$ [4], which is to be compared with $\sigma_{av}=60$ μb for the $(0_1^+,0_2^+)$ channel (see also Refs. [19,20]), whereas the Coulomb penetrabilities differ by a factor of 100.

Among the maxima in the angular distribution of an isolated resonance one would expect that the maximum at 90°

*Permanent address: Faculté des Sciences II, Université Hassan II, Casablanca, Morocco.

has the smallest value (single Legendre polynomial squared). The observed resonancelike structure [4] would be expected to have particular phase shifts in order to exhibit such a strong enhancement around 90°. Indeed, Rae *et al.* [21,22] obtained an excellent fit of the on-resonance angular distributions [4] by assuming that a *shape eigenstate* formed by the *coherent overlap* of states with different l values was excited.

In the earlier investigations of the $^{12}C+^{12}C$ reaction around 32.5 MeV structured excitation functions with a few correlated intermediate-width structures were reported [19,23–26], but a behavior similar to the $(0_2^+,0_2^+)$ data [4] was not observed. The more recent studies of the same $(0_2^+,0_2^+)$ channel [27,28] are not in favor of the simple, apparently coherent shape-eigenstate picture [21,22] that was inspired by the first data set [4]. Integrated over a larger angular range, the excitation function was not consistent with a background-free Breit-Wigner resonance and the shape-eigenstate picture failed to reproduce the on-resonance angular distribution below $\theta_{\text{c.m.}}\approx 40°$ [27].

The recent theoretical investigation of the Kyoto group [29] suggested that the 32.5 MeV resonance was not an isolated phenomenon and that the true physical reality was probably much more complex. Their extended band-crossing model, in which it was assumed that the structure of the underlying excited channels was $3\alpha+3\alpha$ and $3\alpha+^{12}C$ rather than a 6α-chain configuration, predicted an isolated resonant state near 32.5 MeV in the $(0_2^+,0_2^+)$ channel [29]. Without freely adjustable parameters, the on-resonance angular distribution was well reproduced for $\theta_{\text{c.m.}}\geqslant 50°$. The crossing of the ground state and the $(0_2^+,0_2^+)$ bands occurred, however, at $l=18$, which seems not to be supported by a careful analysis of the available experimental angular distributions [30]. At a close energy the ground state band crosses also the $(0_1^+,3_1^-)$ band, the $(0_2^+,3_1^-)$ band, and the $(0_1^+,0_2^+)$ band [29], in accordance with the measurements [20,28] and with the present work.

Surprisingly enough, the $^{12}C+^{12}C\rightarrow{}^{16}O_{\text{g.s.}}+{}^{8}Be_{\text{g.s.}}$ reaction at $E_{\text{c.m.}}=32.5$ MeV exhibited a behavior similar to that of the $(0_2^+,0_2^+)$ channel, although this outgoing channel was hardly reconcilable with the assumed 6α-chain structure of the 32.5 MeV resonance [31–35]. In particular, for the on-resonance angular distribution a large part of the angular range $(50°-90°)$ showed, up to a normalization factor, the same angular dependence as displayed in the inelastic measurement [4,27]. Although the resonance was prominent in both channels, its width differed appreciably: it was only about 1.0 MeV wide for the O+Be channel [34].

The above somewhat confusing and contradictory facts urge for a coherent study of the $^{12}C+^{12}C$ reaction around the resonance at 32.5 MeV by investigating the energy dependence of as many open channels as possible. To insure a safe cross-comparison of different channels, it is preferable to record all the data in the same experiment. We previously performed a measurement of the $^{12}C+^{12}C$ reaction using a kinematic coincidence technique covering also the energy range of the 32.5 MeV resonance [36]. The technique employed responds appropriately to the above requirement. Since the dominant elastic and lower inelastic channels, as well as the strong α-transfer channel have already been analyzed and published [26,34], we have decided to complete the analysis of these data for other discernible open channels in order to contribute to disentangling the 6α-chain state puzzle in ^{24}Mg.

II. EXPERIMENT AND DATA REDUCTION

The present analysis is a reexamination of our previous data on the $^{12}C+^{12}C$ system [26] and presents the measurement hitherto performed with the finest energy step (0.25 MeV) in exploring the excitation functions of this reaction around the putative 6α-chain state at $E_{\text{c.m.}}=32.5$ MeV. The data were collected using the kinematic coincidence technique. Two position-sensitive silicon detectors disposed on either sides of the beam axis were used. One of the detectors subtended the angles $\theta_{\text{lab}}=20°-50°$ and the other $\theta_{\text{lab}}=40°-70°$. The geometry was optimized for the most efficient recording of the main binary channels of the reaction [the elastic and the inelastic scattering to the first excited 2^+ state(s) in ^{12}C]. More details on the conditions of the experiment (beam, target, experimental setup, data recording, analysis, etc.) can be found elsewhere [26,36,37].

The advantage of the kinematic coincidence technique with large position-sensitive detectors lies in the simultaneous detection over a large range of angles of particles coming from different channels. This technique is based on the reaction kinematics in order to determine the masses of reaction products and the reaction Q value.

Figure 1(a) shows the reaction Q-value spectrum constructed from the conservation-of-energy relationship:

$$Q=E_3+E_4-E_{\text{in}} \tag{2.1}$$

obtained with the requirement that each of the detectors should record a particle of energy E_3 and E_4, respectively, within a narrow time window which insures that both particles originate from a single reaction (a coincidence requirement) [36,37]. Here E_{in} is the projectile laboratory energy. The Q spectrum is dominated by three equidistant peaks superimposed on a continuous background. The peaks are due to the particles coming from the elastic scattering, the single inelastic, and the mutually inelastic scattering to the 2^+ state(s) in ^{12}C, respectively. The background is due to the poorly recorded reactions, coming mostly from the incompletely recorded nonbinary channels. A much cleaner Q-value spectrum is obtained when the analysis is limited only to events for which the extracted value for the total mass

$$m_{\text{tot}}=m_3+m_4=\frac{E_{\text{in}}m_p}{\sin^2(\theta_3+\theta_4)}\left(\frac{\sin^2\theta_4}{E_3}+\frac{\sin^2\theta_3}{E_4}\right) \tag{2.2}$$

is $m_{\text{tot}}=24$ a.m.u. In the above relation, m_p stands for the projectile mass and $\theta_3(\theta_4)$ are the deduced angles (positions) at which particles of energy $E_3(E_4)$ were detected. By imposing a given value for m_3 (or, equivalently, for m_4) via Eq. (2.1), the Q-value spectrum is obtained for this particular combination of the outgoing particles, i.e., for a particular binary exit channel. Note, however, that the charge is not detected, so that binary channels with the same mass and similar Q-value spectra cannot be distinguished by the technique applied (see also below for the $^{11}C+^{13}C$ and the ^{11}B

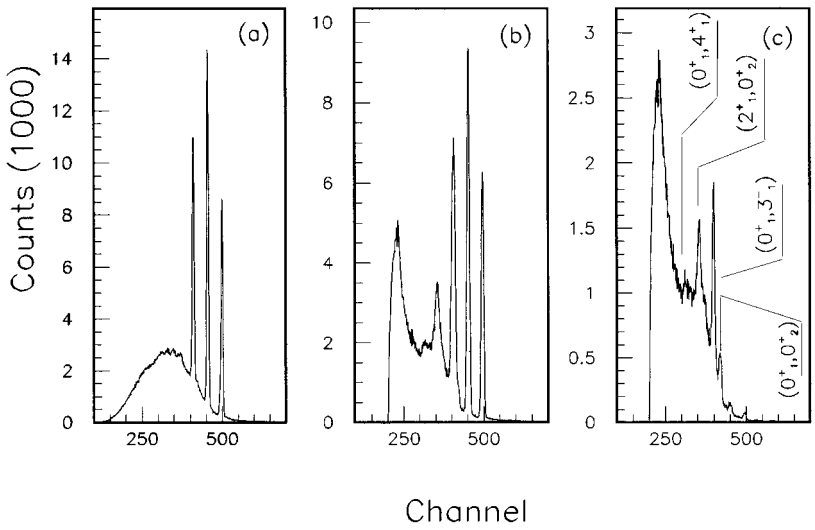

FIG. 1. The Q-value spectra of the $^{12}C+^{12}C$ reaction at the beam energy $E_{in}=33.5$ MeV reconstructed via (a) the unconditioned relationship of energy conservation given by Eq. (2.1), (b) the restrained relationship given by Eq. (2.3), and (c) the relationship given by Eq. (2.3) applied together with the constraint condition on m_{tot} selecting unbound states.

$+^{13}N$ transfer channels). A particularly clean Q-value spectrum is obtained when the dominant elastic/inelastic exit channel is selected via m_3 (or m_4) $=12$ a.m.u. (see Fig. 1 in Ref. [26]).

In the case of a (nearly) monoisotopic target, even nonbinary channels [''background'' in Fig. 1(a)] can be analyzed. Indeed, the undetected particle(s) will carry away part of the total energy. It follows from Eq. (2.2) that this ''missing'' mass gives a false value for the detected m_{tot}, which becomes larger than the actual total mass of the system under study. The strategy is to treat one of the detectors, say, the more-forward-mounted detector (m_3,E_3,θ_3) (which is, normally, kinematically favorable) as the one that correctly detects the particle from a supposed binary channel equivalent to the actual nonbinary channel. In other words, we consider only those particles m_3 which are detected in one of their bound states. By ignoring the data coming from the other detector (i.e., m_4,E_4,θ_4), one can calculate the Q-value spectrum for the particle m_3 in the same way as one would do for an equivalent binary reaction channel. By choosing $m_3=12$ a.m.u., one obtains the following expression for the approximative reaction Q value of the equivalent binary reaction channel:

$$Q_1=2(E_{in}-\cos\theta_3\sqrt{E_{in}E_3}). \tag{2.3}$$

Such a Q_1 spectrum is shown in Fig. 1(b). If one applies Eq. (2.3) only to those events for which Eq. (2.2) gives $m_{tot}>24$, one actually selects nonbinary channels for which one of the particles $(m_3=12)$ is in its bound state. This procedure very efficiently suppresses the elastic and the bound inelastic channels. Now, the weakly excited 0^+_2, 3^-_1, and 4^+_1 (single) inelastic unbound channels emerge from the background and their respective peaks can be readily integrated [Fig. 1(c)]. Although a peak at 12.09 MeV coming from the (mutual) $(2^+_1,0^+_2)$ channel can be discerned, its extraction has not been attempted owing to both its weakness and the complex background dominated by a strong wide peak ($\Gamma=3$ MeV) at 10.3 MeV [5] superimposed on the exponentially rising smooth background.

The Monte Carlo simulation of the detection process was carried out in order to correct the raw data for the complex but weakly energy-dependent relative detection efficiency. It was defined as the ratio of the number of events in which $N\alpha$ particles ($N=1,2,3$) are detected in the less-forward-mounted detector and the number of events in which the $^{12}C[0^+_1]$ nucleus from the primary $^{12}C_{g.s.}+^{12}C^*$ binary scattering was detected in the more-forward-mounted detector. The simulation assumed an isotropic center-of-mass angular distribution for the primary scattering as well as for the subsequent sequential decays $^{12}C^*\rightarrow\alpha+^8Be$ and $^8Be\rightarrow\alpha+\alpha$, where ^8Be was assumed to be in its ground state. Owing to the available small breakup energies for the two subsequent sequential decays (287 and 92 keV, respectively) in the case of the $(0^+_1,0^+_2)$ channel, the average efficiency to detect one or two, out of three emerging α particles, was $70.3-71.6$ % with our detection setup and in the energy range considered. [These processes were relevant to our background-elimination approach, which gave $m_{tot}>24$ via Eq. (2.2).] The probability to detect a full event for this channel was 9.7 (12.3)% for the lowest (highest) energy considered here. The detection probability for the $(0^+_1,3^-_1)$ and $(0^+_1,4^+_1)$ channels was substantially reduced since approximately 2 MeV and 6.5 MeV of additional excitation energies, respectively, were available for the $^{12}C^*$ decay in these two inelastic channels. The α particles were no longer confined within a narrow cone about the recoil direction. The detection efficiency for 1 or 2 α particles was $40.2-44.8$ % for the former and $20.8-24.7$ % for the latter reaction channel. The detection efficiency for the full event dropped down to $1.9-2.7$ % and $0.2-0.5$ %, respectively. Figure 2 displays the detailed angular dependence of the detection efficiency for 1 or 2 α particles as a function of the (referent) angle of the more-forward-mounted detector for the above three channels and $E_{c.m.}=32.5$ MeV. All the data on particle unstable channels presented in this paper, i.e., the inelastic channels and the previously published $^{16}O+^8Be$ [34] rearrangement channels, are corrected for the detection efficiency.

III. RESULTS AND DISCUSSION

In the present work we report on the results of the analysis of weaker channels of the $^{12}C+^{12}C$ reaction between

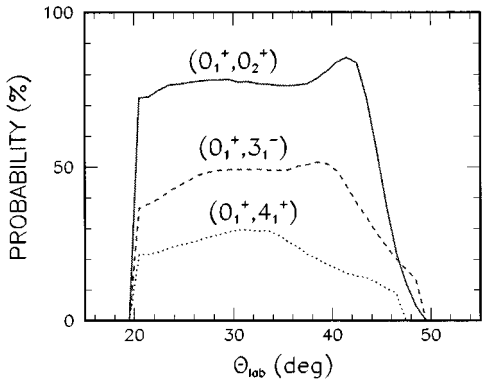

FIG. 2. Angular distributions of the simulated efficiency for detecting either one or two α particles coming from the unbound state of the single inelastic channels $(0_1^+,0_2^+)$, $(0_1^+,3_1^-)$, and $(0_1^+,4_1^+)$ at $E_{\text{c.m.}}=32.5$ MeV.

$E_{\text{c.m.}}=30$ and 35 MeV, in particular of the unbound inelastic channels [38] and the one- and two-nucleon transfer channels. Part of the results extracted in the analysis of the same data were published previously. The results on the elastic scattering and the single and the mutually inelastic scattering to the first excited $^{12}\text{C}[2^+]$ state(s) were reported for the complete data set covering the range $E_{\text{c.m.}}=30-60$ MeV [26]. The analysis of the $^{16}\text{O}+^{8}\text{Be}_{\text{g.s.}}$ rearrangement channel was recently reported [34] for the energy range $E_{\text{c.m.}}=30-35$ MeV.

A. Inelastic channels

The right-hand column of Fig. 3 from top to bottom shows the angle-integrated cross section as a function of energy for the nonbinary (unbound) inelastic channels $(0_1^+,0_2^+)$, $(0_1^+,3_1^-)$, and $(0_1^+,4_1^+)$. To compare our data with the results of Ref. [4], the full angular range $\theta_{\text{c.m.}}=(40°,100°)$ is divided into two parts at about $\theta_{\text{c.m.}}=70°$. Figure 4 from top to bottom shows the integrated cross section for the upper, lower, and full angular range; left for the 0_2^+ and right for the 3_1^- channel. All excitation functions are structured. The integration range is larger than the coherence angle [39]. This strongly suppresses the probability for the observed structure to be of statistical origin.

Two intermediate structures show up, respectively, at $E_{\text{c.m.}}=33.5$ and 32.5 MeV. The structure at 33.5 MeV is correlated for all channels and angular ranges, and its width varies from 0.9 to about 1.6 MeV. The larger-width peak dominates the $(0_1^+,3_1^-)$ [see Fig. 3(e) and right panel of Fig. 4] and $(0_1^+,4_1^+)$ [Fig. 3(f)] excitation functions characterized by peak-to-valley ratios up to 1.5. These two channels display a similar energy dependence, which differs from that for the $(0_1^+,0_2^+)$ channel. The difference is particularly marked when the latter channel is integrated over either the lower [Fig. 4(b)] or the full [Fig. 3(d), Fig. 4(c)] angular range.

The Argonne-group structure observed in the $(0_2^+,0_2^+)$ channel at 32.5 MeV [4] appears in our $(0_1^+,0_2^+)$ data at the same energy but as a narrow, 1.0 MeV wide, peak [Fig. 3(d) or Fig. 4(c)]. When we limit the integration to the angular range of Ref. [4] [Fig. 4(a)], a very wide ($\Gamma>2.5$ MeV) peaklike structure appears. One may speculate that the

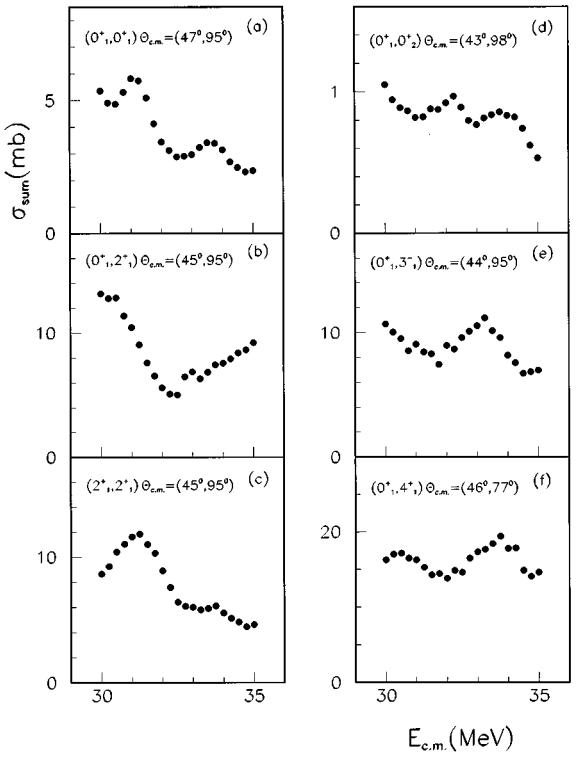

FIG. 3. Angle-integrated excitation functions for (a) the elastic, (b) the single, and (c) the mutually inelastically excited 2^+ state(s) in ^{12}C (left panel) and for the nonbinary (unbound) inelastic channels (d) $(0_1^+,0_2^+)[E_{\text{exc}}=7.65$ MeV], (e) $(0_1^+,3_1^-)[9.64$ MeV], and (f) $(0_1^+,4_1^+)[14.08$ MeV] (right panel).

larger-width peak which we observed in this and other excitation functions is due to the unresolved doublet at 32.5 and 33.5 MeV. All these peaks seem to be encompassed within the strong resonancelike structure of Ref. [4].

Figure 5(a) shows the $(0_1^+,0_2^+)$-channel angular distribution measured at $E_{\text{c.m.}}=32.5$ MeV. It exhibits a regular oscillatory behavior whose maxima and minima are consistent with the $l=14$ squared Legendre polynomial, $[P_{14}(\cos\theta)]^2$. From the figure it is obvious that the $l=12$ (dotted curve), $l=16$ (dashed curve), or $l=18$ (dash-dotted curve) Legendre polynomials cannot account for the data. In the angular range covered by our setup the $(0_1^+,0_2^+)$ angular distribution shows a usual on-resonance shape without enhancement around $\theta_{\text{c.m.}}=90°$. For the sake of comparison, Fig. 5(b) shows the on-resonance angular distribution of the $^{16}\text{O}_{\text{g.s.}}+^{8}\text{Be}_{\text{g.s.}}$ channel in the angular range covered by our setup [33]. This angular distribution displays exactly the same behavior as that of the $^{12}\text{C}[0_2^+]+^{12}\text{C}[0_2^+]$ angular distribution [27]. Although the two distributions shown in Figs. 5(a) and 5(b) are measured at the same energy they differ by the positions of their respective maxima and minima. Furthermore, though the shape of the $^{16}\text{O}_{\text{g.s.}}+^{8}\text{Be}_{\text{g.s.}}$ distribution differs markedly from a single squared Legendre polynomial, the positions of its maxima and minima are exactly those of an $l=16$ squared Legendre polynomial [Fig. 5(b)]. This suggests the dominance of the $l=14$ partial wave in the $(0_1^+,0_2^+)$ outgoing channel and of $l=16$ in the $(0_2^+,0_2^+)$ and the $^{16}\text{O}_{\text{g.s.}}+^{8}\text{Be}_{\text{g.s.}}$ outgoing channels at $E_{\text{c.m.}}=32.5$ MeV.

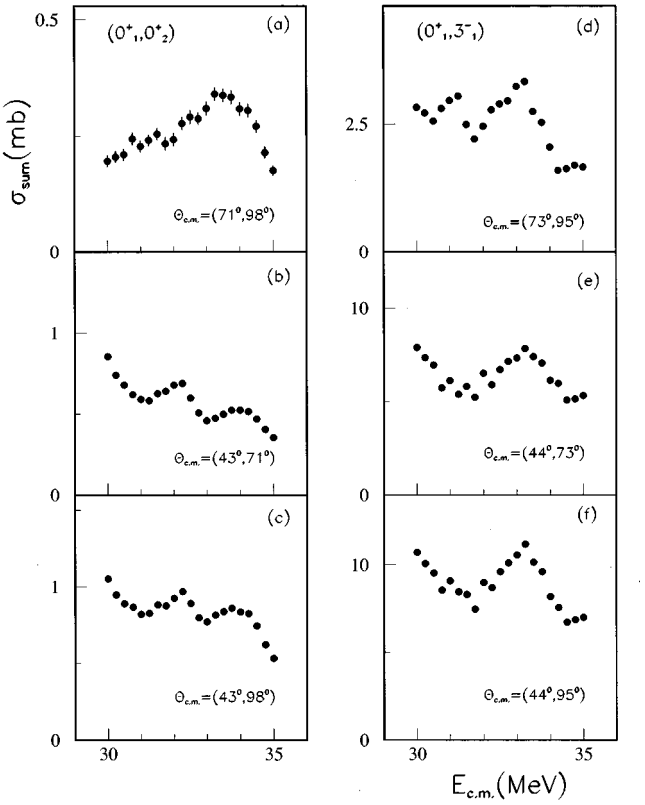

FIG. 4. Excitation functions for the $(0_1^+,0_2^+)$ (left panel) and the $(0_1^+,3_1^-)$ (right panel) inelastic channels integrated over the upper [(a) and (d)], the lower [(b) and (e)], and the whole [(c) and (f)] angular range. The integration limits are indicated in the figure.

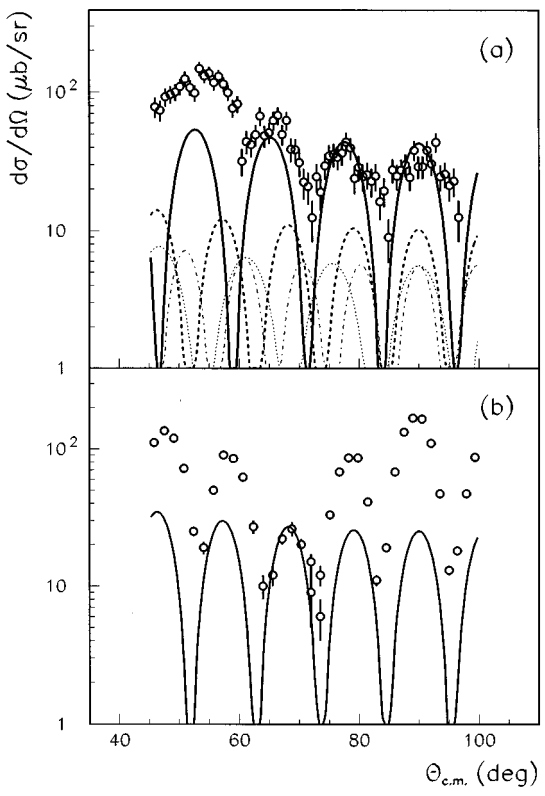

FIG. 5. Angular distributions of (a) the $^{12}C(^{12}C,^{12}C[0_1^+])^{12}C[0_2^+]$ inelastic scattering and (b) the $^{12}C(^{12}C,^{16}O_{g.s.})^8Be_{g.s.}$ reaction at $E_{c.m.}=32.5$ MeV. Shown are also the squared Legendre polynomials of the degree $l=14$ (solid curve), $l=16$ [dashed curve in (a) and solid curve in (b)], $l=12$ (dotted curve), and $l=18$ (dash-dotted curve).

Resonancelike behavior is evident in the same energy range in the elastic [Fig. 3(a)] and the mutually excited inelastic channels [Fig. 3(c)] [26]. The intermediate structure at 33.5 MeV has a width and a peak-to-valley ratio that are similar to the width and the peak-to-valley ratio obtained in our work. (We remind the reader that these data come from the same experiment.) The correlation of the structure observed at 33.5 MeV in at least four channels speaks in favor of a genuine resonance. A complete list of the observed intermediate structures in the elastic and inelastic channels is given in Table I.

The integrated excitation function for the $(0_1^+,3_1^-)$ channel and measured for more forward angles ($\theta_{c.m.}=33°-55°$) was reported in Ref. [19]. It showed resonancelike structure at 33 MeV. In the energy range of interest in this paper, some much weaker structure can also be discerned in the $(0_1^+,0_2^+)$ and $(0_1^+,4_1^+)$ channels.

The angle-integrated excitation functions have recently been studied for a few $^{12}C^*+^{12}C^*$ channels [28]. The excitation functions for the $(0_2^+,0_2^+)$ and $(0_2^+,3_1^-)$ channels show strong resonancelike structure in the region $E_{c.m.}=32.5$ MeV. In the $(3_1^-,3_1^-)$ and $[0_2^+,(1^-)]$ channels a less pronounced doubletlike behavior appears peaking at 32.5 and 35 MeV, respectively.

In their recent work [40] the Argonne group has reported on a strong resonance in the $(0_1^+,3_1^-)$ channel at $E_{c.m.}=33.5$ MeV.

B. Transfer channels

The large negative reaction Q value is the reason why there are only a few studies of the one- and two-nucleon transfer channels of the $^{12}C+^{12}C$ system. In this paper we present the excitation functions for the main rearrangement channels, namely, the one-nucleon transfer channels ($^{11}C_{g.s.}+^{13}C_{g.s.}$ and/or $^{11}B_{g.s.}+^{13}N_{g.s.}$) and the two-nucleon transfer channel ($^{10}B_{g.s.}+^{14}N_{g.s.}$). As discussed in Sec. II,

TABLE I. Intermediate structures observed in the elastic and inelastic channels of the $^{12}C+^{12}C$ reaction between center-of-mass energies of 30 and 35 MeV.

$E_{c.m.}$ [MeV]	$(0_1^+,0_1^+)$	$(0_1^+,2_1^+)$	$(2_1^+,2_1^+)$	$(0_1^+,0_2^+)$	$(0_1^+,3_1^-)$	$(0_1^+,4_1^+)$
$-Q$ [MeV]	0.00	4.44	8.88	7.65	9.65	14.05
31.0	yes	no	yes	no	no	no
32.5	no	no	no	yes	no	no
33.5	yes	no	yes	yes	yes	yes

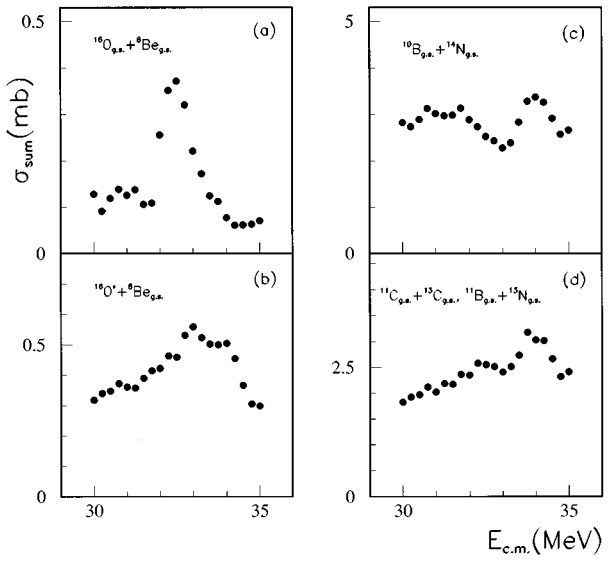

FIG. 6. Integrated excitation functions of (a) $^{16}O_{g.s.}+^{8}Be_{g.s.}$, (b) $^{16}O^{*}+^{8}Be_{g.s.}$ to the group of unresolved states in ^{16}O around an excitation energy of $6-7$ MeV, and (c) the one- and (d) the two-nucleon transfer channels.

we are not able to distinguish channels having the same mass and similar Q values. The ground-state Q values for the $m_3=13$ channels differ only by 0.24 MeV; this value is smaller than our resolution. Therefore, both one-nucleon transfer reactions contribute to the reported excitation function. The conventional analysis with expressions (2.1) and (2.2) was performed by taking $m_3=13$ and $m_3=14$, respectively. Since the experimental setup was optimized to detect the main binary channels, a somewhat more limited angular range was covered for the masses $m_3=13$ ($50° \leqslant \theta_{c.m.} \leqslant 95°$) and $m_3=14$ ($51° \leqslant \theta_{c.m.} \leqslant 99°$).

The right panel in Fig. 6 shows the angle-integrated cross section for the transfer channels. The main feature of the excitation functions is a strong resonancelike peak centered at 34 MeV with a width of about 1 MeV. In comparison with the structure of the unbound inelastic channels presented in the preceding subsection, this peak is slightly shifted (less than the peak width) towards higher energy. The width and peak-to-valley ratios of the structure are the same. The structure at about 31 MeV is less convincing and appears only for the $^{10}B+^{14}N$ channel [Fig. 6(c)]. Some nonconclusive irregularity can be observed in the $m_3=13$ data at 32.5 MeV [Fig. 6(d)].

The prominent, well-matched rearrangement channel is the $^{16}O+^{8}Be$ α-transfer channel. Although the $^{16}O_{g.s.}+^{8}Be_{g.s.}$ excitation function of Ref. [34] [Fig. 6(a)] was integrated over the same angular range as in Ref. [4], the reported isolated narrow peak ($\Gamma=1.0$ MeV) at 32.5 MeV had the characteristics of our $(0_1^+,0_2^+)$ data in the full angular range [Fig. 3(d)] rather than the characteristics of the $(0_2^+,0_2^+)$ excitation function [4]. The same strong isolated narrow peak is reported for the same channel and the same angular range in Ref. [35]. These $^{16}O_{g.s.}+^{8}Be_{g.s.}$ excitation functions show no sign of structure at 33.5 MeV, the energy at which we observe strongly correlated peak. On the contrary, the $^{16}O^{*}+^{8}Be_{g.s.}$ excitation function for a group of unresolved states around 6–7 MeV in ^{16}O exhibits a strong wide doubletlike structure centered at 33.5 MeV [Fig. 6(b)]. A complete list of the intermediate structures observed in the transfer channels is given in Table II.

The transfer-channel excitation functions were measured by the Rochester group covering a more forward angular range ($\theta_{c.m.}=23°-51°$) [24,25]. Strong structure was reported for the angle-integrated data at 31 MeV for the $^{10}B_{g.s.}+^{14}N_{g.s.}$ channel and at 33 MeV for the $^{10}B[1^+]+^{14}N_{g.s.}$ channel. At 32.5 MeV a peak could be observed only in those excitation functions which were measured at the most forward angles. The differences observed in the transfer excitation functions might come from the different angular range of integration covered in Refs. [24,25] and in our measurement.

IV. CONCLUSIONS

The present data show that the region of the 32.5 MeV resonance is more complex than indicated by the initial experiment [4]. We have analyzed the $^{12}C+^{12}C$ reaction between $E_{c.m.}=30-35$ MeV. Coming from the same experiment, all excitation functions of the outgoing channels studied previously (elastic, $(2_1^+,2_1^+)$ mutually inelastic [26], and $^{16}O+^{8}Be_{g.s.}$ transfer channels [34]) and presently [$(0_1^+,0_2^+)$, $(0_1^+,3_1^-)$, and $(0_1^+,4_1^+)$ inelastic and $^{11}C_{g.s.}+^{13}C_{g.s.}$, $^{11}B_{g.s.}+^{13}N_{g.s.}$, and $^{10}B_{g.s.}+^{14}N_{g.s.}$ transfer channels] display correlated intermediate-width structures (see Tables I and II). In the energy range studied, intermediate structures are not observed only in the $(0_1^+,2_1^+)$ channel [26].

Within the width of the putative 6α-chain state [4] we observe three intermediate-width structures at $E_{c.m.}=31$, 32.5, and 33.5 MeV, which are correlated in most of the channels studied (see Tables I and II). The extended band-crossing model is able to qualitatively explain the behavior observed in the inelastic channels [29]. The complexity of the structure at $E_{c.m.}=32.5$ MeV is clearly evident from the angular distributions of the resonating channels involving zero-spin nuclei. The on-resonance angular distribution of

TABLE II. Intermediate structures observed in the one- and two-nucleon and α-particle transfer channels of the $^{12}C+^{12}C$ reaction between center-of-mass energies of 30 and 35 MeV.

$E_{c.m.}$ [MeV]	$^{11}C_{g.s.}+^{13}C_{g.s.}$ $^{11}B_{g.s.}+^{13}N_{g.s.}$	$^{10}B_{g.s.}+^{14}N_{g.s.}$	$^{8}Be+^{16}O_{g.s.}$	$^{8}Be+^{16}O^{*}$
$-Q$ [MeV]	13.78–14.01	14.9	0.21	6.26–7.33
32.5	yes	no	yes	yes
33.5	yes	yes	no	yes

the $^{12}C[0_1^+]+^{12}C[0_2^+]$ channel is consistent with an $l=14$ [Fig. 5(a)], whereas the on-resonance angular distributions of the $^{12}C[0_2^+]+^{12}C[0_2^+]$ and the $^{16}O_{g.s.}+^{8}Be_{g.s.}$ outgoing channels [Fig. 5(b)] reveal a mixture of many partial waves with the dominant effect on the oscillatory behavior coming from the last contributing wave, $l=16$ [30]. These data argue for the conclusion that at 32.5 MeV the $^{12}C+^{12}C$ entrance channel populates a complex structure at an excitation energy of 46.4 MeV in ^{24}Mg. From this structure the $^{12}C[0_2^+]+^{12}C[0_2^+]$ and the $^{16}O_{g.s.}+^{8}Be_{g.s.}$ outgoing channels pick up one particular configuration that is different from that which decays through the $^{12}C[0_1^+]+^{12}C[0_2^+]$ channel.

The outgoing flux is unequally distributed among channels. The Q value and the channel spin matching play an important role. For instance, the average angle-integrated cross section for the $(0_1^+,4_1^+)$ $[(0_1^+,3_1^-)]$ channel is about 20 (10) times larger than that of the $(0_1^+,0_2^+)$ channel.

Since the band-crossing model has proved its worth for predicting the energy and angular dependence of a number of inelastic channels, it would be interesting to make a detailed comparison between the model calculations and the present data. The comparison will be even more valuable if the transfer channels could be incorporated in the model. We hope that this new piece of data will encourage the theorists of the Kyoto group to reexamine their calculation in the light of the new experimental findings.

ACKNOWLEDGMENTS

It is a pleasure to thank our colleagues from the LNS, Catania, and in particular M. Zadro from the RBI, Zagreb, for making their experimental angular distributions available to us. Two of us (S.S. and Z.B.) would like to express their gratitude to the Centre de Recherche Nucléaires and Université Louis Pasteur, Strasbourg, for the warm hospitality during their stay. One of us (S.S.) would like to express her gratitude to the French Government for financial support.

[1] N. Cindro, Nuovo Cimento **4**, 1 (1981).
[2] N. Cindro, Ann. Phys. (Paris) **13**, 289 (1988).
[3] W. Greiner, J. Y. Park, and W. Scheid, *Nuclear Molecules* (World Scientific, Singapore, 1995).
[4] A. H. Wuosmaa, R. R. Betts, B. B. Back, M. Freer, B. G. Glagola, Th. Happ, D. J. Henderson, P. Wilt, and I. G. Bearden, Phys. Rev. Lett. **68**, 1295 (1992).
[5] F. Ajzenberg-Selove, Nucl. Phys. **A506**, 1 (1990).
[6] H. Morinaga, Phys. Rev. **101**, 254 (1956).
[7] H. Morinaga, Phys. Lett. **21**, 78 (1966).
[8] D. M. Brink, H. Friedrich, A. Weiguny, and C. W. Wong, Phys. Lett. **33B**, 143 (1970).
[9] H. Friedrich, L. Satpathy, and A. Weiguny, Phys. Lett. **36B**, 189 (1971).
[10] N. Takigawa and A. Arima, Nucl. Phys. **A168**, 593 (1971).
[11] Y. Suzuki, H. Horiuchi, and K. Ikeda, Prog. Theor. Phys. **47**, 1517 (1972).
[12] E. Uegaki, S. Okabe, Y. Abe, and H. Tanaka, Prog. Theor. Phys. **57**, 1262 (1977).
[13] M. Kamimura, Nucl. Phys. **A351**, 456 (1981).
[14] G. Leander and S. E. Larsson, Nucl. Phys. **A239**, 93 (1975).
[15] N. Cindro and W. Greiner, J. Phys. G **9**, L175 (1983).
[16] S. Marsh and W. D. M. Rae, Phys. Lett. **180B**, 185 (1986).
[17] Z. Basrak, W. Tiereth, N. Bischof, H. Fröhlich, B. Nees, E. Nieschler, and H. Voit, Phys. Rev. C **32**, 910 (1985).
[18] Z. Basrak, W. Tiereth, and H. Voit, Phys. Rev. C **37**, 1511 (1988).
[19] B. R. Fulton, T. M. Cormier, and B. J. Herman, Phys. Rev. C **21**, 198 (1980).
[20] S. F. Pate, R. W. Zurmühle, P. H. Kutt, and A. H. Wuosmaa, Phys. Rev. C **37**, 1953 (1988).
[21] W. D. M. Rae, A. C. Merchant, and B. Buck, Phys. Rev. Lett. **69**, 3709 (1992).
[22] A. C. Merchant and W. D. M. Rae, J. Phys. G **19**, L89 (1993).
[23] T. M. Cormier, C. M. Jachcinski, G. M. Berkowtz, P. Braun-Munzinger, P. M. Cormier, M. Gai, J. W. Harris J. Barrette, and H. E. Wegner, Phys. Rev. Lett. **40**, 924 (1978).
[24] M. R. Clover, T. M. Cormier, B. R. Fulton, and B. J. Herman, Phys. Rev. Lett. **43**, 256 (1979).
[25] T. M. Cormier and B. R. Fulton, Phys. Rev. C **22**, 565 (1980).
[26] A. Morsad, F. Haas, C. Beck, and R. M. Freeman, Z. Phys. A **338**, 61 (1991).
[27] A. H. Wuosmaa, M. Freer, B. B. Back, R. R. Betts, J. C. Gehring, B. G. Glagola, Th. Happ, D. J. Henderson, P. Wilt, and I. G. Bearden, Phys. Rev. C **50**, 2909 (1994).
[28] S. P. G. Chappell *et al.*, Phys. Rev. C **51**, 695 (1995).
[29] Y. Hirabayashi, Y. Sakuragi, and Y. Abe, Phys. Rev. Lett. **74**, 4141 (1995).
[30] R. M. Freeman *et al.* (unpublished).
[31] M. Aliotta, S. Cherubini, E. Costanzo, M. Lattuada, S. Romano, C. Spitaleri, D. Vinciguerra, and M. Zadro, Nucl. Phys. **A583**, 281c (1995).
[32] E. T. Mirgule, Suresh Kumar, M. A. Eswaran, D. R. Chakrabarty, V. M. Datar, N. L. Ragoowansi, H. H. Oza, and U. K. Pal, Nucl. Phys. **A583**, 287c (1995).
[33] M. Aliotta, S. Cherubini, E. Costanzo, M. Lattuada, S. Romano, D. Vinciguerra, and M. Zadro, Z. Phys. A **353**, 43 (1995).
[34] R. M. Freeman, F. Haas, A. Elanique, A. Morsad, and C. Beck, Phys. Rev. C **51**, 3504 (1995).
[35] M. Aliotta, S. Cherubini, E. Costanzo, M. Lattuada, S. Romano, C. Spitaleri, A. Tumino, D. Vinciguerra, and M. Zadro, Z. Phys. A **354**, 119 (1996).
[36] A. Morsad, Ph.D. Thesis, University of Strasbourg, 1985.
[37] R. M. Freeman, C. Beck, F. Haas, A. Morsad, and N. Cindro, Phys. Rev. C **33**, 1275 (1986).
[38] All but the ground state and the first excited 2^+ state at 4.44 MeV in the ^{12}C nucleus are particle unbound.
[39] P. Braun-Munzinger and J. Barrette, Phys. Rev. Lett. **44**, 719 (1980).
[40] A. H. Wuosmaa, R. R. Betts, and M. Freer, Argonne National Laboratory Annual Report No. ANL-95/14 (unpublished), p. 13.